PHYSICAL REVIEW B VOLUME 40, NUMBER 17 15 DECEMBER 1989-I

# Effects of disorder on electronic structures of *a*-Si:H and *a*-SiO$_2$

Jeyasingh Nithianandam and Stephen E. Schnatterly
*Jesse Beams Laboratory of Physics, University of Virginia, Charlottesville, Virginia 22901*

(Received 13 February 1989)

Si $L_{23}$ x-ray emission spectra from *c*-Si, doped and intrinsic *a*-Si:H, quartz, and *a*-SiO$_2$ are presented. The first and second moments of the valence-band transition density of states of each of these samples were computed. The variance of the disorder potential that characterizes the amorphous network was found for the amorphous samples from their second moments. Lifetime broadening as a function of energy in the valence band of silicon samples was found to vary significantly between the crystalline and amorphous structures.

The electronic properties of crystalline and amorphous phases of silicon and silicon dioxide have been extensively studied by different experimental and theoretical methods.[1] Amorphous materials differ from crystalline materials as they lack long-range order, possessing bond-length and bond-angle disorders. In this work we use amorphous silicon and silicon dioxide for testing theories of localized band-tail states that arise due to intrinsic disorder in amorphous solids. Soft-x-ray emission spectroscopy (SXES) provides direct information on the occupied valence-electron states of solids. We used the method of moments[2] with SXES in the study of localized electron states in *a*-Si:H and *a*-SiO$_2$. In this work we report the first direct estimate of degree of disorder and width of valence-band (VB) tail of *a*-Si:H and *a*-SiO$_2$ with x-ray emission spectroscopy.

The description of our SXE spectrometer is given elsewhere.[3] The SXE spectra were excited by bombardment of the sample with an electron beam of 1–3 keV energy. The soft-x-ray photons emitted due to electronic transitions from occupied valence or conduction states to the vacancy in the Si 2*p* core level were energy dispersed by a toroidal grating and detected by a position-sensitive photodiode array detector. The energy resolution of our SXE spectrometer is about 0.1 eV. Device quality films of undoped, phosphorus doped, and boron doped *a*-Si:H and *a*-SiO$_2$ which were grown on *c*-Si substrates by a chemical vapor deposition (CVD) process were obtained from the Exxon Research and Engineering Company. The *n*-type *a*-Si:H (*p*-type *a*-Si:H) was made by mixing 2% phosphine (2% diborine) with silane in the CVD apparatus. The thickness of the *a*-Si:H samples was 1–2 $\mu$m and the *a*-SiO$_2$ sample was 3000 Å thick.

The *L* x-ray emission spectrum of silicon has unwanted contributions from effects like self-absorption, shakeup, and bremsstrahlung. Livins and Schnatterly showed that a wide hump centered at about 80.3 eV below the VB edge in the raw *L* x-ray emission spectrum of *c*-Si is mainly due to shakeup contributions.[4] They showed that the shakeup intensity contributions in the silicon *L* x-ray emission spectrum roughly has the shape of an asymmetric Lorentzian function which is damped on the high-energy side. The procedure for removing shakeup contributions from the *L* x-ray emission spectrum of *c*-Si has been discussed in detail elsewhere.[5] We briefly outline this procedure here. The lower VB edge of the *L* x-ray emission spectrum of *c*-Si can be described by a square-root function convoluted with a Lorentzian function whose full width at half maximum (FWHM) varies as $C(E_\gamma - E)^2$, where $C$ is a constant and $E_\gamma$ is about one band gap below the VB maximum. We added an asymmetric Lorentzian function to describe shakeup contributions and a straight line for background intensity from bremsstrahlung. A nonlinear least-squares curve fitting routine based on this model was used to fit the raw data of *c*-Si and *a*-Si:H between 65 and 88.5 eV allowing us to remove the shakeup intensity contributions from the raw *L* x-ray emission spectra.

Self-absorption effects influence the *L* x-ray emission spectra of silicon near the Si $L_{23}$ absorption threshold region. Crisp developed an algorithm to correct x-ray emission spectra for these effects.[6] We obtained *L* x-ray emission spectra from *a*-Si:H at 1- and 3-keV electron beam excitation energies and used the Crisp algorithm to correct the *a*-Si:H data for self-absorption effects. The x-ray emission spectra of silicon were finally transformed into TDOS by dividing by $E^3$, where $E$ is the photon energy, and normalization of the spectrum to an area of unity between 68 and 103 eV. The valence-band transition density of states (VBTDOS) of the silicon samples are shown in Fig. 1. The details of data acquisition from crystalline quartz and *a*-SiO$_2$ samples and subsequent data reduction were described in our earlier work. The valence x-ray emission bands of *c*-SiO$_2$ and *a*-SiO$_2$ obtained with a 1.5-keV electron beam are shown in Fig. 2.

Soft-x-ray emission spectra of semiconductors and insulators resemble a series of peaks and hence it is tempting to fit them with a small number of line-shape functions. Using a spectral synthesis method described in detail elsewhere,[7–10] the shapes of the *L* x-ray emission spectra of *c*-Si and *a*-Si:H samples in the energy range 82–99 eV were simulated by a suitable combination of six Voigt functions. The Voigt profile results from the convolution of a Lorentzian and a Gaussian line shape.[8] We present these results without any presumption that either the Lorentzian or Gaussian components have any physi-

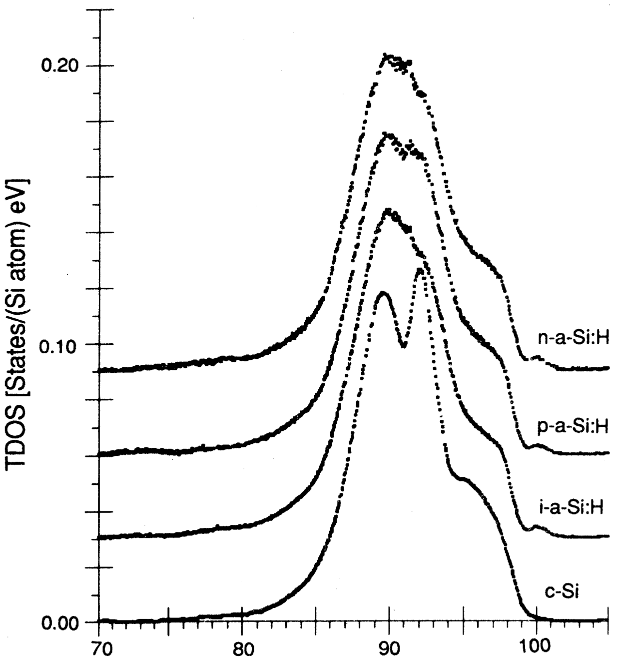

FIG. 1. *L* x-ray emission spectra from silicon samples. The area under each of the emission bands has been normalized to unity.

cal meaning. We shall argue below, however, that the Lorentzian component does have meaning. The parameters of our multipeak fit to the TDOS of the crystalline and amorphous silicon obtained from these emission spectra are shown in Table I. The values of the multipeak fit parameters summarized in Table I will allow others to reproduce our data in a convenient and accurate manner. Figure 3 shows a multipeak fit to the *L* x-ray emission spectrum of undoped *a*-Si:H.

Disorder in amorphous semiconductors modifies the electronic spectra, especially near the valence- and conduction-band edges, where tails in the DOS are produced below these band edges.[11–13] The localized electron states in the valence- and conduction-band tails could be responsible for the Urbach edge observed in the optical spectra of amorphous semiconductors.[9–13] Moreover, these band-tail states dominate charge transport and conduction in these solids. The properties of these band-tail states have been extensively studied by experimental[14–16] and theoretical[17–20] methods. In one theoretical approach in the study of disordered systems,[21] the Hamiltonian of an amorphous solid is estimated by adding a randomly fluctuating potential to the crystalline Hamiltonian. We denote the difference between the crystalline and amorphous Hamiltonians by *V*. The Anderson model introduces *V* as a Gaussian distribution of random potentials at each crystalline potential well. We obtained the mean value $\langle V \rangle$ and the variance $\langle V^2 \rangle$ of the random potential of *a*-Si:H and *a*-SiO$_2$ from their valence x-ray emission bands by the method of moments described below. The quantities defined by the expressions

$$\mu_k=\int_{-\infty}^{\infty} E^k N(E)dE \tag{1a}$$

are called moments of the density of states, $N(E)$ and $E$ is the photon energy. These moments[2] can be written as

$$\mu_k=\mathrm{Tr}(H^k)=\sum_{i_0}\langle i_0|H^k|i_0\rangle \;, \tag{1b}$$

where $|i_0\rangle$ represents an orbital of the solid and so mo-

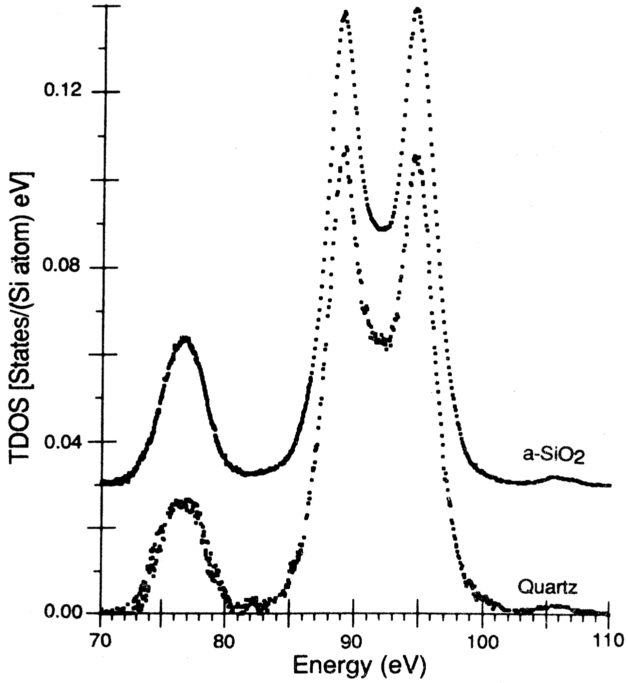

FIG. 2. Si *L* x-ray emission band from crystalline quartz and amorphous-silicon dioxide.

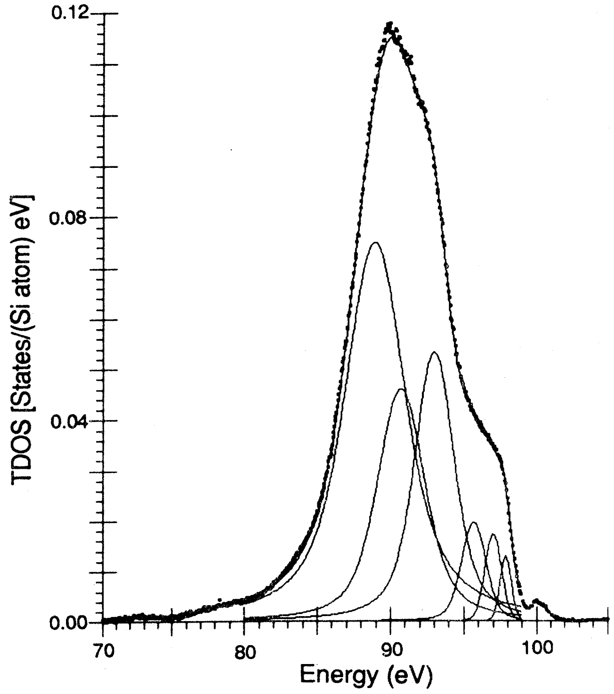

FIG. 3. Fit to the valence-band x-ray emission spectrum of intrinsic *a*-Si:H with six broadened line-shape functions.

TABLE I. Parameters of multipeak fit to the valence-band emission spectra of silicon samples. $E_i$ is the position of the peak. $\Gamma_g$ and $\Gamma_l$ are the full width at half maximum (FWHM) of the Gaussian and Lorentzian parts of the Voigt profile in eV. $N(E_i)$ is the intensity at the peak in transition density of states (TDOS) units and $A(E_i)$ is the area of the peak in units of states/(Si atom) between 80.5 and 99 eV.

(a) Peaks from fit to *c*-Si data

| Parameters | *A* | *B* | *C* | *D* | *E* | *F* |
|---|---|---|---|---|---|---|
| $E_i$ | 89.46 | 91.8 | 92.51 | 94.10 | 96.17 | 97.69 |
| $\Gamma_g$ | 2.67 | 0.26 | 1.25 | 2.72 | 2.39 | 1.44 |
| $\Gamma_l$ | 2.85 | 0.95 | 0.55 | 0.0 | 0.043 | 0.011 |
| $N(E_i)$ | 0.11 | 0.033 | 0.055 | 0.026 | 0.031 | 0.013 |
| $A(E_i)$ | 0.653 | 0.054 | 0.106 | 0.075 | 0.078 | 0.02 |

(b) Peaks from fit to undoped *a*-Si:H data

| Parameters | *A* | *B* | *C* | *D* | *E* | *F* |
|---|---|---|---|---|---|---|
| $E_i$ | 88.93 | 90.7 | 92.97 | 95.64 | 96.97 | 97.83 |
| $\Gamma_g$ | 2.8 | 2.68 | 2.17 | 1.7 | 1.31 | 0.9 |
| $\Gamma_l$ | 3.11 | 1.81 | 1.58 | 0.47 | 0.055 | 0.014 |
| $N(E_i)$ | 0.075 | 0.046 | 0.053 | 0.02 | 0.017 | 0.013 |
| $A(E_i)$ | 0.458 | 0.215 | 0.21 | 0.044 | 0.025 | 0.012 |

(c) Peaks from fit to P-doped *a*-Si:H data

| Parameters | *A* | *B* | *C* | *D* | *E* | *F* |
|---|---|---|---|---|---|---|
| $E_i$ | 88.85 | 90.82 | 92.98 | 95.66 | 96.93 | 97.82 |
| $\Gamma_g$ | 3.11 | 2.76 | 2.45 | 1.89 | 1.53 | 1.14 |
| $\Gamma_l$ | 2.65 | 1.63 | 1.51 | 0.26 | 0.002 | 0.002 |
| $N(E_i)$ | 0.076 | 0.045 | 0.052 | 0.02 | 0.017 | 0.013 |
| $A(E_i)$ | 0.451 | 0.204 | 0.213 | 0.045 | 0.028 | 0.015 |

(d) Peaks from fit to B-doped *a*-Si:H data

| Parameters | *A* | *B* | *C* | *D* | *E* | *F* |
|---|---|---|---|---|---|---|
| $E_i$ | 89.04 | 90.93 | 92.59 | 95.58 | 97.02 | 97.87 |
| $\Gamma_g$ | 2.72 | 4.12 | 2.36 | 2.35 | 1.48 | 0.98 |
| $\Gamma_l$ | 3.28 | 1.72 | 1.47 | 0.096 | 0.023 | 0.017 |
| $N(E_i)$ | 0.068 | 0.037 | 0.052 | 0.022 | 0.017 | 0.013 |
| $A(E_i)$ | 0.452 | 0.218 | 0.208 | 0.056 | 0.027 | 0.014 |

ments $\mu_k$ of the DOS are diagonal elements of successive powers of the Hamiltonian of the solid. In SXES we measure the transition density of states and so instead of DOS, we use $f_c(E)$ and $f_a(E)$ the TDOS distributions of crystalline and amorphous phases of a solid to compute moments and these TDOS distributions are written as follows:

$$f_c(E)=|\langle\phi|x|\phi_0\rangle|^2 N_c(E)\ , \tag{2a}$$

$$f_a(E)=|\langle\psi|x|\psi_0\rangle|^2 N_a(E)\ . \tag{2b}$$

Here, $N_c(E)$ and $N_a(E)$ are the VBDOS of crystalline and amorphous phases of a solid, respectively. The dipole matrix elements in Eq. (2) govern the x-ray transitions from the valence-band states $|\phi\rangle$ and $|\psi\rangle$ to the core states $|\phi_0\rangle$ and $|\psi_0\rangle$ of crystalline and amorphous materials, respectively. The first moments $\mu_{1c}$ and $\mu_{1a}$ of the TDOS distributions of crystalline and amorphous phases of these solids are then given by the following expressions:

$$\mu_{1c}=\bar{E}_c=\int_{E_l}^{E_m} E f_c(E)dE\ , \tag{3a}$$

$$\mu_{1a}=\bar{E}_a=\int_{E_l}^{E_m} E f_a(E)dE\ . \tag{3b}$$

The VBTDOS of silicon in Fig. 1 has negligible contributions below 80.5 and above 98.6 eV and so we set $E_l=80.5$ eV and $E_m=98.6$ eV. We set $E_l=72.0$ eV and $E_m=97.7$ eV for $SiO_2$. We then obtain[22]

$$\bar{E}_a \simeq \bar{E}_c+\langle V\rangle\ . \tag{4}$$

The second moments $\mu_{2c}$ and $\mu_{2a}$ of the TDOS of crystalline and amorphous phases of a solid about energy position $\bar{E}_c$ are written as follows:

$$\mu_{2c}=\langle (E-\bar{E}_c)^2\rangle_c=\int_{E_l}^{E_m}(E-\bar{E}_c)^2 f_c(E)dE\ , \tag{5a}$$

$$\mu_{2a}=\langle (E-\bar{E}_c)^2\rangle_a=\int_{E_l}^{E_m}(E-\bar{E}_c)^2 f_a(E)dE\ . \tag{5b}$$

The second moments of crystalline and amorphous phases of a solid are related to each other by

$$\mu_{2a} \simeq \mu_{2c} + \langle V^2 \rangle . \tag{6}$$

We numerically computed the first and second moments of the VBTDOS distributions of silicon and silicon dioxide using Eqs. (3)–(6) and these values are shown in Table II.

John and collaborators[18] constructed from first principles the DOS in the energy band tail for an electron in a Gaussian random potential of an amorphous solid. They obtained a linear exponential dependence of the DOS $\rho(E)$ on the energy which can be expressed as

$$\rho(E) \sim \exp(-|E|/W) \tag{7a}$$

with

$$W = \frac{V_{\rm rms}^2}{14.4 E_L} . \tag{7b}$$

Here, $W$ is the width of the band tail and $E_L = \hbar^2/2mL^2$ is the energy associated with localizing an electron of mass $m$ within the correlation length $L$. The correlation length in $a$-Si:H is estimated to be of the order of the interatomic spacing which is 2.35 Å.[23] We used $\langle V^2 \rangle$ obtained from our second moment calculations for $V_{\rm rms}^2$ in Eq. (7b) and found the width of the VB tail for $i$-type $a$-Si:H, $p$-type $a$-Si:H, and $n$-type $a$-Si:H to be 58, 59, and 84 meV, respectively.[24]

There is no theoretical estimate to our knowledge about the correlation length in $a$-SiO$_2$. The Si-Si and O-O nearest-neighbor distances are 3.06 and 2.63 Å, respectively.[24] Neutron scattering measurements[25] yield radial distribution function maxima for $a$-SiO$_2$ at 3.5 and 4.2 Å. If we assume the correlation length to be about 3 Å for $a$-SiO$_2$, then using Eq. (7b) we obtain a value of 0.81 eV for the width of the valence-band tail of $a$-SiO$_2$.

A nonlinear least-squares program based on a simple model described in detail in our previous work[7] was used to fit the $L$ x-ray emission spectra of $a$-Si:H sample in the region 97.5–102.5, which includes the top of the VB, the band-gap region, and the bottom of the conduction band. Crisp and co-workers[26] have claimed that the upper valence-band edge of the $L$ x-ray emission spectrum of $a$-Si:H has parabolic shape consistent with an effective-mass description.[27] We used a Gaussian broadening function of FWHM $\Gamma_G$ convoluted with the function $A_t(E_t - E)^{0.5}$ and used the resulting function $B(E)$ to describe the observed upper valence-band edge of the $L$ x-ray emission spectrum of $a$-Si:H. Here, $E_t$ is the position of the top of the VB and $A_t$ is a constant. We used an exponential energy band-tail function convoluted with the Gaussian broadening function for the shape of the DOS near the VB maximum of $a$-Si:H and this function $T(E)$ is joined to the function $B(E)$ so as to best fit the data. It was found that inclusion of the exponential tail function $T(E)$ in the curve fitting routine helped to improve the fit to the $a$-Si:H data in this energy region, however the same can be said for the $c$-Si data so we are forced to conclude that the excess emission above the top of the valence band is not dominated by band-tail states and must have another physical origin.

The emission higher in the gap region is presumably due to the Si 2$p$ core exciton and defect states. We used in our fit a Voigt line-shape function for the defect states and core exciton. Thus our model for $a$-Si:H in the gap region includes $B(E)$, $T(E)$, and two Voigt functions. We included a spin-orbit splitting value of 0.61 eV and allowed the $L_2/L_3$ intensity ratio to be a variable parameter and this ratio was found to be nearly 0.5 for the fits to the $a$-Si:H data. A model fit to the $L$ x-ray emission spectrum of P-doped $a$-Si:H for states at the top of the VB and in the gap region is shown in Fig. 4. The values of the parameters of the model are shown in Table III. In the case of $a$-SiO$_2$ we used a straight line $A_t(E_t - E)$ for the upper VB edge and the results were reported in our earlier work on SiO$_2$.[28]

Winer and co-workers directly observed an exponential energy band tail and dangling-bond defect states in $a$-Si:H using total yield photoelectron spectroscopy.[14,15] Theoretical work[29] predicts dangling-bond defect states at 1.4 eV below the conduction band of $a$-Si:H. Stutzmann and collaborators[30] suggest that the dangling-bond defect states in $a$-Si:H could be due to breaking of weak Si—Si bonds which lie just above the VB edge. The peak at 98.6 eV in the fit to $n$-type $a$-Si:H shown in Fig. 4 could be due to the dangling bonds or weak bonding states above the VB edge. The peak at 99.9 eV is due to the Si 2$p$ core exciton as it is near the Si $L_{23}$ absorption threshold.[31] The dangling-bond defect states are 1.3 eV below the Si 2$p$ core exciton. The band gap of $a$-Si:H is

TABLE II. Moments of the TDOS of silicon and silicon dioxide samples and calculated values of the widths of the valence-band exponential tail of amorphous samples. $\langle V \rangle$ and $\langle V^2 \rangle$ are the mean value and the mean square value of random potential, respectively, of amorphous samples. $\bar{E}_c$ is the first moment of the valence-band TDOS of crystalline sample and $E_L$ is the energy associated with localizing an electron within the correlation length. $W$ is the width of the valence-band tail in amorphous samples.

| Sample | $E$ eV | $\langle (E-\bar{E}_c)^2 \rangle$ eV$^2$ | $\langle V \rangle$ eV | $\langle V^2 \rangle$ eV$^2$ | $W = \langle V^2 \rangle/(14.4E_L)$ eV |
|---|---|---|---|---|---|
| $c$-Si | 90.98 | 11.27 | | | |
| $i$-type $a$-Si:H | 90.77 | 11.84 | −0.21 | 0.57 | 0.058 |
| $p$-type $a$-Si:H | 90.87 | 11.85 | −0.11 | 0.58 | 0.059 |
| $n$-type $a$-Si:H | 90.78 | 12.1 | −0.2 | 0.83 | 0.084 |
| $c$-SiO$_2$ | 89.76 | 33.49 | | | |
| $a$-SiO$_2$ | 89.34 | 38.39 | −0.42 | 4.9 | 0.81 |

TABLE III. Model fit parameters to upper valence-band edge and gap region of $a$-Si:H samples. $E_t$ is the position of valence-band maximum ($L_3$) in eV. $A_t$ is the multiplicative constant in the square-root function of the valence-band edge in units of [states/eV$^{1.5}$ (Si atom)]. $\Gamma_G$ is the FWHM of Gaussian broadening function in eV. $M$ is the energy position at which the $B(E)$ function joins the $T(E)$ function. $W$ is the width of the valence-band exponential tail in eV. $N_t$ is the number of (states/Si atom) at $M$. $\Gamma_{V_1}$ and $\Gamma_{V_2}$ are the FWHM of the Voigt functions in eV.

(a) Model fit parameters to upper valence-band edge of $a$-Si:H

| | | | Parameters | | | |
|---|---|---|---|---|---|---|
| Sample | $E_t$ | $A_t$ | $\Gamma_G$ | $M$ | $W$ | $N_t$ |
| $i$-type $a$-Si:H | 98.36 | 0.038 | 0.497 | 98.42 | 0.106 | $2.9\times10^{-5}$ |
| $n$-type $a$-Si:H | 98.38 | 0.043 | 0.49 | 98.5 | 0.086 | $4.5\times10^{-6}$ |
| $p$-type $a$-Si:H | 98.39 | 0.048 | 0.44 | 98.42 | 0.064 | $2.2\times10^{-7}$ |

(b) Model fit parameters to gap region of $a$-Si:H

| | | | Parameters | | | | |
|---|---|---|---|---|---|---|---|
| Sample | $E_1$ | $\Gamma_{V_1}$ | $N(E_1)$ | $E_2$ | $\Gamma_{V_2}$ | $N(E_2)$ | $\chi^2$ |
| $i$-type $a$-Si:H | 98.58 | 1.08 | 0.0012 | 99.93 | 0.96 | 0.003 | 15.6 |
| $n$-type $a$-Si:H | 98.55 | 0.55 | 0.0029 | 99.87 | 1.17 | 0.003 | 2.2 |
| $p$-type $a$-Si:H | 98.55 | 0.63 | 0.0025 | 99.94 | 1.03 | 0.0025 | 6.4 |

1.77 eV (Ref. 32) and so the core exciton binding energy is 0.2 eV.

Crandall, using photocurrent measurements in $a$-Si:H structures, determined the absorption coefficient and obtained information about the density of VB tail states.[33] He obtained 90 meV for the width of the VB tail of undoped $a$-Si:H and 100 meV for P-doped $a$-Si:H. Cody and co-workers[16] using optical absorption measurements on $a$-Si:H obtained a value of 70 meV for the width of the valence-band tail. Total yield photoelectron spectroscopy, which is a surface-sensitive experimental technique, gives a value of 45 meV for the widths of the VB tails of undoped and B-doped $a$-Si:H.[14,15] The value of $W$ for $i$-type $a$-Si:H, $n$-type $a$-Si:H, and $p$-type $a$-Si:H obtained from the moments of the VBTDOS are in excellent agree-

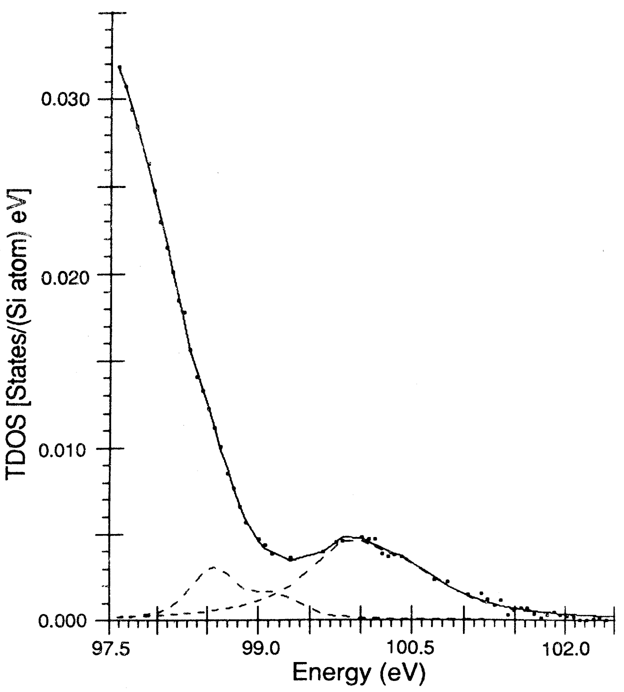

FIG. 4. The valence-band edge and gap region part of the $L$ x-ray emission spectrum of $n$-type $a$-Si:H and fit based on a model described in the text.

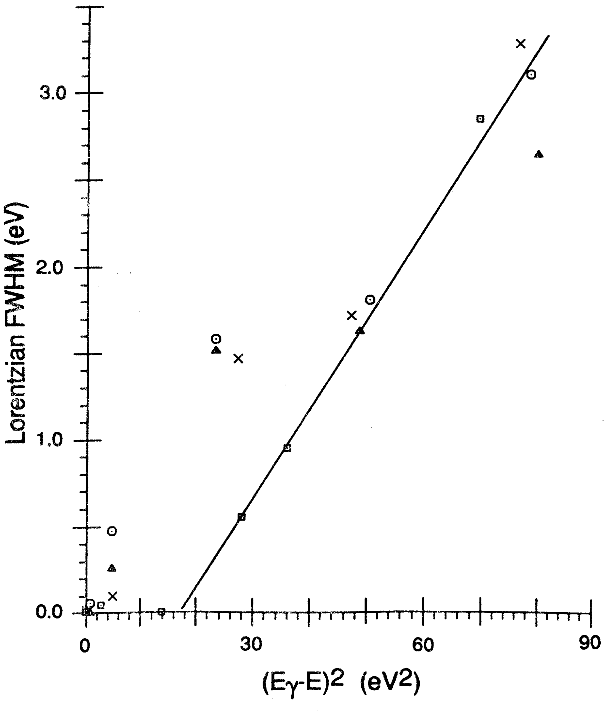

FIG. 5. Lifetime broadening as a function of energy in the valence band of silicon samples. $\Gamma_l$ is the FWHM of the Lorentzian part of the Voigt components of the valence band in eV. Squares, circles, triangles, and crosses correspond to $c$-Si, $i$-type $a$-Si:H, $n$-type $a$-Si:H, and $p$-type $a$-Si:H samples.

ment with other reported moments, and if our input values for the parameters in Eq. (7) for $a$-Si:H are correct, then our results support the validity of the theory of John[18] on the exponential energy band tails.

Frölich suggested the occurrence of an internal Auger effect that introduces a Lorentzian broadening contribution to the VB electron states observed in the x-ray emission spectrum of a solid.[34] The hole left in the VB due to the radiative transition of an electron to the vacant core level (here Si $2p$ core level) has a finite lifetime due to the electron-electron interaction. An electron at a higher VB level fills this VB vacancy and gives up its energy to a second electron which is promoted to an unoccupied electron state in the conduction band. Landsberg showed that the level width $\Gamma_l$, arising from this internal Auger effect, decreases from the bottom of the VB to the top of the VB where it vanishes.[34] This level width $\Gamma_l$ was found[35] to vary roughly as $(E_\gamma - E)^2$. The threshold energy $E_\gamma$ in the VB lies at an energy of about 1 band gap below the VB maximum.

The values of the Lorentzian FWHM $\Gamma_l$ from the multipeak fit to the VBTDOS of $c$-Si and $a$-Si:H are shown in Table I. These values may represent the lifetime broadening of the valence electron states or they may have no physical meaning at all. To pursue this question, in Fig. 5 we have plotted the Lorentzian widths $\Gamma_l$ of the six Voigt components of $c$-Si and $a$-Si:H as a function of $(E_\gamma - E)^2$, where we have set $E_\gamma = 97.8$ eV. The systematic variation of the $\Gamma_l$ values with $E$ suggests that these values actually represent valence hole lifetime broadening. The values of $\Gamma_l$ near the bottom of the valence band agree well with earlier results.[4] Apparently the Gaussian component of the broadening describes the shape of the TDOS sufficiently well that the Lorentzian component is dominated by the actual lifetime broadening. In $c$-Si the $\Gamma_l$ values remain quite small, within 4–5 eV of the VB top, and then rise quadratically. Apparently the Si $3p$-$3p$ Auger matrix element is small compared with the $3s$-$3s$ values. In $a$-Si:H the $\Gamma_l$ values rise rapidly from the VB top, suggesting that the $3s$ and $3p$ states are thoroughly mixed.

The authors wish to thank Dr. B. Abeles of Exxon Research and Engineering Corporation for amorphous silicon and silicon dioxide samples. The authors acknowledge Professor S. John of Princeton University, Professor C. M. Soukoulis of Iowa State University, and Professor W. Y. Ching of University of Missouri for useful discussions and also acknowledge the other members of our laboratory, R. D. Carson, P. Bruhwiler, D. Husk, C. Tarrio, S. Valesquez, and E. Benetiz for their help throughout the course of this work. This work was supported in part by National Science Foundation Grant No. DMR-85-15684.

---

[1] S. R. Elliott, *Physics of Amorphous Materials* (Longman, London, 1984).

[2] F. Yndurain and F. J. Yndurain, J. Phys. C **8**, 434 (1975).

[3] R. D. Carson, C. P. Frank, S. E. Schnatterly, and F. Zutavern, Rev. Sci. Instrum. **55**, 1973 (1984).

[4] P. Livins and S. E. Schnatterly, Phys. Rev. B **37**, 6731 (1988).

[5] P. A. Bruhwiler, Ph.D. thesis, University of Virginia, 1988.

[6] R. S. Crisp, J. Phys. F **13**, 1325 (1983).

[7] V. J. Nithianandam and S. E. Schnatterly, Phys. Rev. B **36**, 1159 (1987).

[8] D. G. Hummer, Mem. R. Astron. Soc. **70**, 1 (1955).

[9] B. G. Cartling, J. Phys. C **8**, 3171 (1975).

[10] V. Hietschold and G. Seifert, Phys. Status Solidi B **129**, K163 (1985).

[11] B. von Roedern, L. Ley, and M. Cardona, Phys. Rev. Lett. **39**, 1576 (1977).

[12] E. N. Economou and D. A. Papconstantopoulos, Phys. Rev. B **23**, 2042 (1981).

[13] E. Z. Kurmaev and G. Weich, J. Non-Cryst. Solids **70**, 187 (1985).

[14] K. Winer and L. Ley, Phys. Rev. B **36**, 6072 (1987).

[15] K. Winer, I. Hirabayashi, and L. Ley, Phys. Rev. Lett. **60**, 2697 (1988).

[16] G. D. Cody, T. Tiedje, B. Abeles, B. Brooks, and Y. Goldstein, Phys. Rev. lett. **47**, 1480 (1981).

[17] Y. Bar-Yam, D. Adler, and J. D. Joannopoulos, Phys. Rev. Lett. **57**, 467 (1986).

[18] S. John, C. Soukoulis, M. H. Cohen, and E. N. Economou, Phys. Rev. Lett. **57**, 1777 (1986).

[19] J. Singh, Phys. Rev. B **23**, 4156 (1981).

[20] W. Y. Ching, Phys. Rev. Lett. **46**, 607 (1981).

[21] N. F. Mott and E. A. Davis, *Electronic Process in Non-Crystalline Materials* (Clarendon, Oxford, 1979).

[22] F. J. Zutavern, Ph.D. thesis, Princeton University, 1982.

[23] V. Sa-Yakanit and H. R. Glyde, Comments Condensed Matter Phys. **13**, 35 (1987).

[24] F. J. Grunthaner and P. J. Grunthaner, Mater. Sci. Rep. **1**, 65 (1986).

[25] L. Guttman and S. M. Rahman, Phys. Rev. B **37**, 2657 (1988).

[26] R. S. Crisp, D. Haneman, and V. Chacorn, J. Phys. C **21**, 975 (1988).

[27] S. Kivelson, and C. D. Gelatt, Jr., Phys. Rev. B **19**, 5160 (1979).

[28] V. J. Nithianandam and S. E. Schnatterly, Phys. Rev. B **38**, 5547 (1988).

[29] J. D. Joannopoulos, J. Non-Cryst. Solids **35-36**, 781 (1980).

[30] M. Stutzmann, D. K. Biegelsen, and R. A. Street, Phys. Rev. B **35**, 5666 (1987).

[31] F. C. Brown, R. Z. Bachrach, and M. Skibowski, Phys. Rev. B **15**, 4781 (1977).

[32] B. Abeles and T. Tiedje, Phys. Rev. Lett. **51**, 2003 (1983).

[33] R. S. Crandall, Phys. Rev. Lett. **44**, 749 (1980).

[34] J. Pirenne and P. Longe, Physica **30**, 277 (1964).

[35] H. J. Levinson, F. Greuter, and E. W. Plummer, Phys. Rev. B **27**, 727 (1983).